J Mater Sci: Mater Med (2009) 20:521–527
DOI 10.1007/s10856-008-3610-3

Human osteoblasts adhesion and proliferation on magnesium-substituted tricalcium phosphate dense tablets

Marcia S. Sader · Racquel Z. LeGeros · Gloria A. Soares

Received: 20 June 2008 / Accepted: 2 October 2008 / Published online: 6 November 2008

Abstract Tricalcium phosphate (TCP) is recognized as a promising bone replacement material due to its high bioactivity and resorbable properties. To mimic biological apatites, incorporation of magnesium (Mg) in TCP was proposed. Mg-substituted TCP (β-TCMP) and β-TCP dense tablets were obtained by pressing and sintering at 1,000°C Mg-substituted calcium deficient apatite (Mg-CDA) and commercial TCP, respectively. The materials were characterized using X-ray diffraction, infrared spectroscopy and electron microscopy. Human osteoblast cells (SaOs2) were seeded onto the sintered tablets for 4 h, 24 h and 7 days. Results showed that Mg-CDA was completely transformed into β-TCMP. Moreover, β-TCMP stimulated adhesion and proliferation of human osteoblast cells. Consequently, the magnesium incorporation on calcium deficient apatites followed by sintering at 1,000°C seems to be a useful path to obtain biocompatible and non cytotoxic dense tablets with TCP structure with potential application on bone engineering.

1 Introduction

The osteoconductive and resorbable properties of tricalcium phosphate (β-TCP) make it attractive for use, alone or togheter with hydroxyapatite (HA), as bone substitutes and as a starting material for bone cement. Its low solubility and high bioactivity permit this material to be replaced by newly formed bone allowing its use in regenerative medicine [1].

TCP has been studied to overcome the low biodegradability of hydroxyapatite. The solubility of HA at physiological conditions depends mainly on its crystallinity and the incorporation of some ions to approximate the properties of biological apatites. Biological apatites are characterized by nano-crystal sizes, low crystallinity, nonstoichiometry and several ionic substitutions, such as Mg-for-Ca, CO_3-for-PO_4 [2, 3].

Tricalcium phosphate (TCP) or whitlockite, $Ca_3(PO4)_2$, is characterized by a Ca/P ratio of 1.5. TCP can not be precipitated by aqueous conditions due to its instability in water. It is usually obtained through the synthesis of calcium-deficient apatite and subsequent calcination in the range of 700–800°C to form the allotropic form β-TCP with loss of water [1, 4, 5].

Magnesium (Mg) is one of the most important bivalent ions associated with biological tissue. Mg deficiency affects all skeletal metabolism stages causing cessation of bone growth, decrease of osteoblastic and osteoclastic activities, osteopenia and bone fragility [6]. Magnesium easily replaces calcium in the apatite lattice enhancing the nucleation rate of apatite crystal and inhibiting its crystallization. Mg, in biological systems, appears to stabilize the whitlockite or β-TCP structure. This apparent stabilizing effect in β-TCMP is due to the increased electrostatic bonding of Mg–O vs. Ca–O in the structure and the closer distances between Mg–O compared to Ca–O in the Mg-substituted whitlockite structure [7]. Mg affects the stability of the lattice, causing a decrease in the unit-cell parameters and consequently in crystallite size and/or increase in crystal strain [8]. Mg incorporated in apatite lattice increases its solubility [2, 9].

M. S. Sader · G. A. Soares (✉)
Metallurgical and Materials Department, COPPE/UFRJ,
Rio de Janeiro, RJ, Brazil
e-mail: gloria@metalmat.ufrj.br

R. Z. LeGeros
New York University College of Dentistry,
New York, NY, USA

Magnesium-substituted TCP (β-TCMP) can be obtained either by wet precipitation method from several precursors, pH, temperature and molar ratio Mg/Ca or by hydrolysis of dicalcium phosphate dihydrate (DCPD), $CaHPO_4 \cdot 2H_2O$ or dicalcium phosphate anhydrate, DCPA, $CaHPO_4$ in solutions with varying Mg/Ca molar ratios [8, 10]. A final product, with a uniform particle size, without residual second phases is obtained when the wet precipitation method is employed, making this process efficient for the fabrication of powders, granules, dense and porous bodies and for coatings of metallic or polymeric implants [11].

In vitro studies are often used to verify the biocompatibility and biomaterial interaction with cells. Zreiqat [12] suggested that surface modification of bioceramics with Mg^{2+} resulted in an osteoblasts adhesion increase via higher expression levels of integrin receptors. Magnesium ions seem to contribute to cell detection on the surface of apatite crystals throughout integrin action, which exist on the cell membrane, confirming the acceleration effect of bone formation by magnesium [13].

The aim of this work was to verify the effect of the magnesium introduction in the calcium deficient apatite lattice in the human osteoblast cells response (adhesion and proliferation) and compare to the β-TCP one of commercial origin.

2 Materials and methods

Mg-substituted calcium deficient apatite, Mg-CDA, was synthesized by precipitation method from an aqueous solution of calcium hydroxide 1.25 M, [$Ca(OH)_2$], containing magnesium chloride 0.24 M, [$MgCl_2.6H_2O$], and orthophosphoric acid 2.8 M, [H_3PO_4], at 39°C, pH = 9. The precipitate was aged for 24 h at 25°C, washed, filtered, dried overnight at 40°C and sieved at 125 µm.

The synthesized Mg-containing material was compared with a commercial product labeled as tricalcium phosphate, (Merck, dried extra pure, Darmstadt, Ge). Part of both materials was uniaxially pressed in cylindrical tablets (13 mm diameter and 1 mm height) under compressive strength of 216 MPa, followed by sintering at 1,000°C for 4 h in air (2.8°C/min heating rate). The geometric densities of the sintered tablets were calculated and the resultant surface microporosity was examined by scanning electron microscopy SEM (JEOL, JSM6460LV).

The specific surface area of the non-sintered powders was determined by BET method (Micrometrics, ASAP 2010). The Mg-CDA green powder was analyzed by transmission electron microscopy, TEM, (JEOL, 2000FX) to verify crystal morphology and size. TEM sample was prepared by dispersing Mg-CDA powder in ethanol bath with ultrasonic vibration. Few drops were deposited on a TEM copper grid, coated with a formvar and carbon films. The qualitative chemical composition was assessed by energy dispersive spectroscopy, EDS, (Thermo/System Six, model 100).

Both materials (green powder and sintered tablets, with and without Mg) were characterized by X-ray diffraction (XRD) and Fourier-transform infrared spectroscopy (FTIR). For these analyses, the sintered tablets were crushed and sieved. XRD Rietveld analyses were performed with Bragg-Brentano geometry, using XPERT PRO XRD equipment (Panalytical), CuKα radiation, 40 kV and 40 mA. The absorption bands of the materials were obtained using FTIR spectroscopy (ABB Bomem Inc., MB series), recorded in the range of 400 to 4,000 cm^{-1}.

To evaluate osteoblasts adhesion and proliferation, 4×10^4 cells/well of human osteoblasts (SaOs2) were seeded onto the tablets for 4 h, 24 h and 7 days. For each point time 4 samples of each condition were tested. After incubation period, samples were fixed and examined by SEM.

3 Results and discussion

The specific surface areas of the green powders were 199 m^2/g and 57 m^2/g for Mg-CDA and β-TCP, respectively. The high specific surface area of Mg-substituted Ca deficient apatite (Mg-CDA) is compatible with the nanometric particle sizes showed on TEM micrograph. Figure 1a shows the bright field image of needle-like crystals with approximately 150 nm of length. EDS analyses (Fig. 1b) of these crystals confirmed the presence of Mg.

The XRD pattern of the green and sintered Mg-CDA samples can be seen on Fig. 2. The XRD profile of green powder showed an apatite with very low crystallinity, mixed with tricalcium phosphate phase. After sintering, the Mg-CDA sample was completely transformed into whitlockite magnesian phase (JCPDS 13-0404 card). The high specific surface area of the Mg substituted apatite increased the surface reactivity allowing the total conversion of Mg-CDA to β-TCMP.

On Fig. 3, the XRD profile of as-received commercial TCP powder was ascribed as an apatite with low crystallinity mixed with another phase (non identified) but after sintering at 1,000°C the transformation into pure β-TCP (JCPDS 09-0169 card) was completed.

The Mg substitution on apatite lattice decreases the crystal size as shown by the broadening of the diffraction peaks of the Mg-CDA green powder when compared with as-received TCP powder. The shifts of diffraction peaks to higher 2θ values confirmed the partial substitution of Mg-for-Ca in the whitlockite structure, β-TCMP,

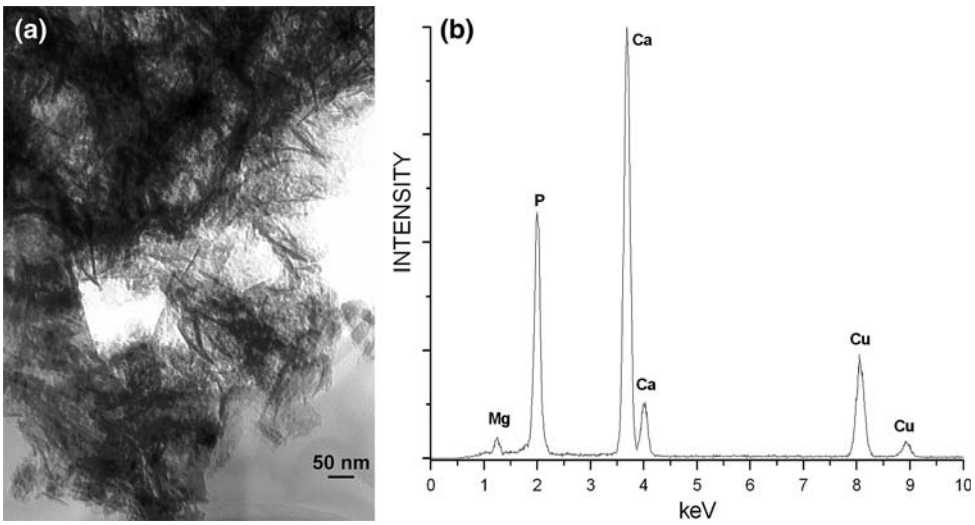

Fig. 1 **a** TEM micrograph of Mg-CDA and **b** the EDS spectrum

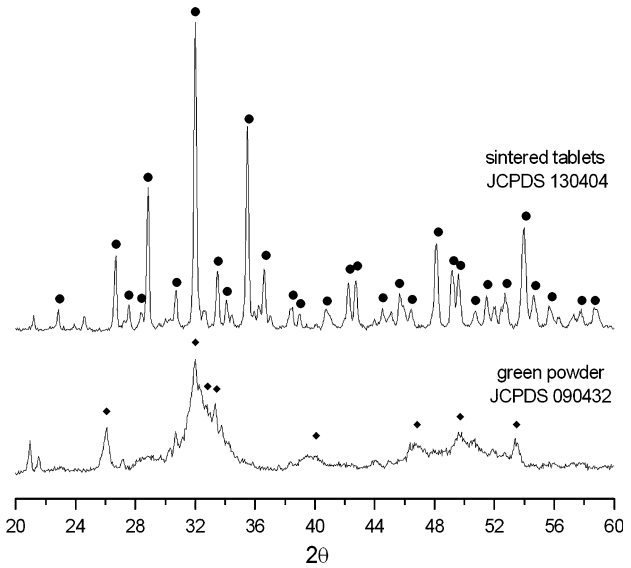

Fig. 2 XRD diffraction profiles of Mg-CDA: **a** before and **b** after sintering at 1,000°C

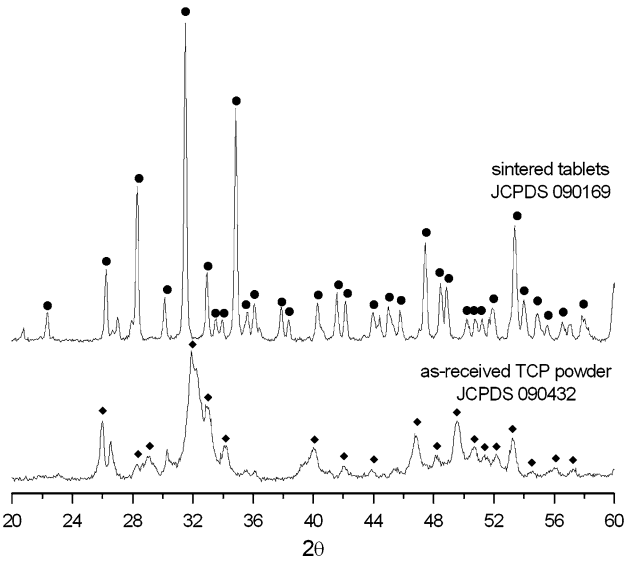

Fig. 3 XRD diffraction profiles of commercial TCP **a** as-received and **b** after sintering at 1,000°C

$(Ca, Mg)_3(PO_4)_2$. It indicates a contraction in the unit cell dimensions caused by the partial substitution of $Mg^{2+}$with smaller ionic radius for the Ca^{2+} [2, 8]. The lattice parameters of the unit cell were calculated by Rietveld analyses and showed on Table 1. The parameters a = b and c as well as the unit cell volume decreased with the incorporation of Mg on Ca deficient apatite.

The occupancy values obtained from the Rietveld refinement were used to estimate quantitatively the insertion of the Mg^{2+} in the Ca deficient apatite lattice. The Mg inclusion on β-TCMP occupied 24% of the positions of Ca (4) site and 87% of Ca (5) site. The limit value of Mg that enters in the structure as Ca substitute was around 11%, leading to approach the molecular formula as $Ca_{2.70}\left(Mg^{V}_{0.23}Mg^{IV}_{0.07}\right)(PO_4)_2$

Table 1 Lattice parameters and unit cell volume of the sintered samples

Sample	$a = b$(nm)	c (nm)	V(nm^3)
β-TCP	1.04208(2)	3.73711(7)	3.514
β-TCMP	1.03229(0)	3.72066(0)	3.433

The different modes of vibrations and rotations of functional groups can be observed in the corresponding FTIR spectra of the green and sintered samples presented on Fig. 4. FTIR spectra of the green powders show broad bands of water (at 3,440 and 1,639 cm^{-1}) attributed to the wet precipitation process used to obtain the samples. The band at 874 cm^{-1} can be seen in both green samples and can be attributed to HPO_4^{-2}, which is characteristic of

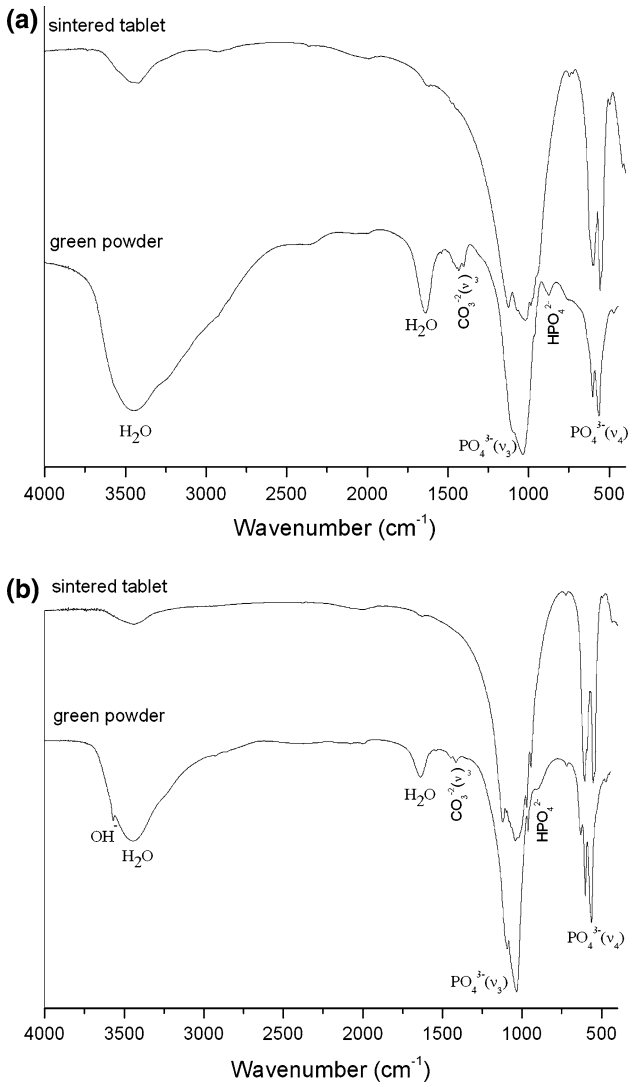

Fig. 4 FTIR spectra of: **a** the Mg-CDA (green and sintered tablets) and **b** the commercial TCP (as received and sintered tablets)

calcium deficient apatite. The sintering process resulted in the disappearance of the hydrogenphosphate absorption band and a decrease in the water bands intensity. The phosphate band (v_3 PO_4^{3-}) at 1035 cm^{-1} changed into three peaks better resolved in the sintered samples. The lack of resolution of the v_3 PO_4^{3-} band also indicates low crystallinity. The phosphate bands (v_4 PO_4^{3-}) at 603 and 564 cm^{-1} are present in all spectra. Carbonate bands ($v_3CO_3^{-2}$) in the range of 1,400–1,450, characteristic of Type B CO_3 substitution in the apatite (CO_3-for-PO_4), are only seen in the green samples spectra. They can be attributed to the process of synthesis, which was not done under inert atmosphere. The characteristic OH^- bands at 3,570 and 631 cm^{-1} can be seen only in the commercial TCP (as received). The Mg incorporation on the apatite lattice decreases the crystallite size and the degree of atomic disorder increase within the apatite unit cell, which favored the low degree of hydroxylation [14].

The compacting behavior of the powders was very different. The tablets produced from Mg-CDA exhibited higher volumetric contraction after sintering as well as higher densification compared to the commercial β-TCP tablets. The geometric densities for the tablets after sintering were 2.45 ± 0.04 g/cm^3 and 1.83 ± 0.04 g/cm^3 for β-TCMP and commercial β-TCP, respectively. The lattice parameters decreasing could explain the contraction effect of the Mg-CDA tablets.

Due to the different level of densification, a surface microporosity variation was observed. Actually, a lower microporosity can be observed on β-TCMP when compared to commercial β-TCP (Fig. 5). In order to obtain β-TCP tablets without significant porosity, Santos et al. [15] used higher sintering temperature (1,150°C), but he could not avoid excessive grain size growth. According to Lin et al. [16], low temperature sintering is an effective way to obtain high-density bodies with fine grain size.

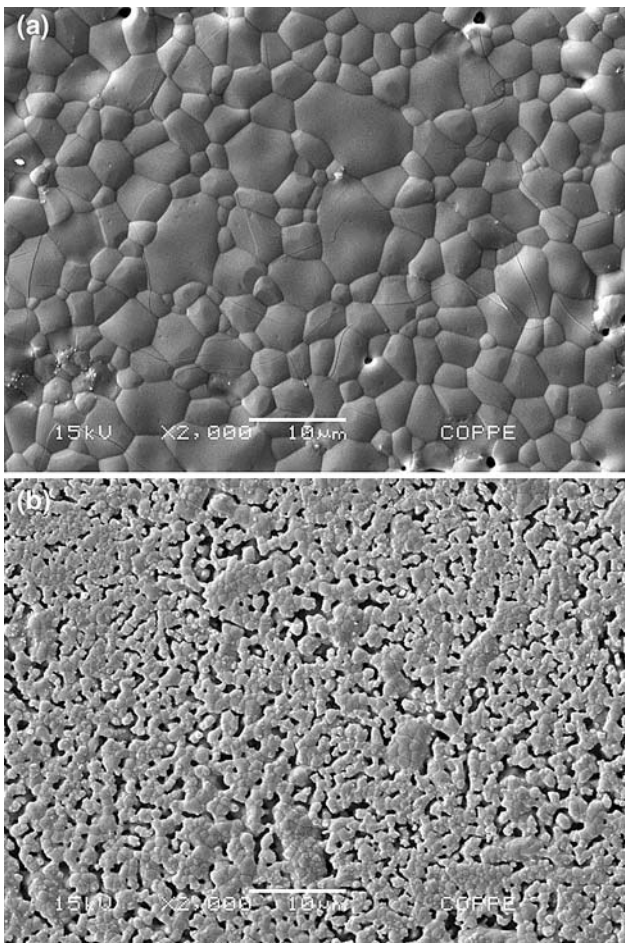

Fig. 5 SEM images of tablets sintered at 1,000°C: **a** β-TCMP; **b** commercial β-TCP

The initial adhesion stages and proliferation of human osteoblasts cultured on β-TMCP and on commercial β-TCP tablets were evaluated by SEM, as shown in Fig. 6. After 4 h of incubation, a small number of non-spreading spherical osteoblasts were observed on both tablets, with lower number of cells observed on β-TCMP. After 24 h of incubation, the cell density on β-TCMP increased. Osteoblast cells adhered and spread on both samples after 7 days of incubation, but the adhesion and spreading rates were different. The cells were widely spread and adhered to the β-TCMP substrate exhibiting a flattened attachment with long filopodia extended in all directions. Figure 7 presents a monolayer of cells recovering all the surface of the β-TCMP tablet after 7 days.

The biomaterial surface modification, in terms of topography and/or chemistry, can affect the phenotype of osteogenic cells both in vivo and in vitro tests and influence the protein adhesion process affecting the cell adhesion and proliferation. The cellular interaction between osteoblasts and the biomaterial is mediated by

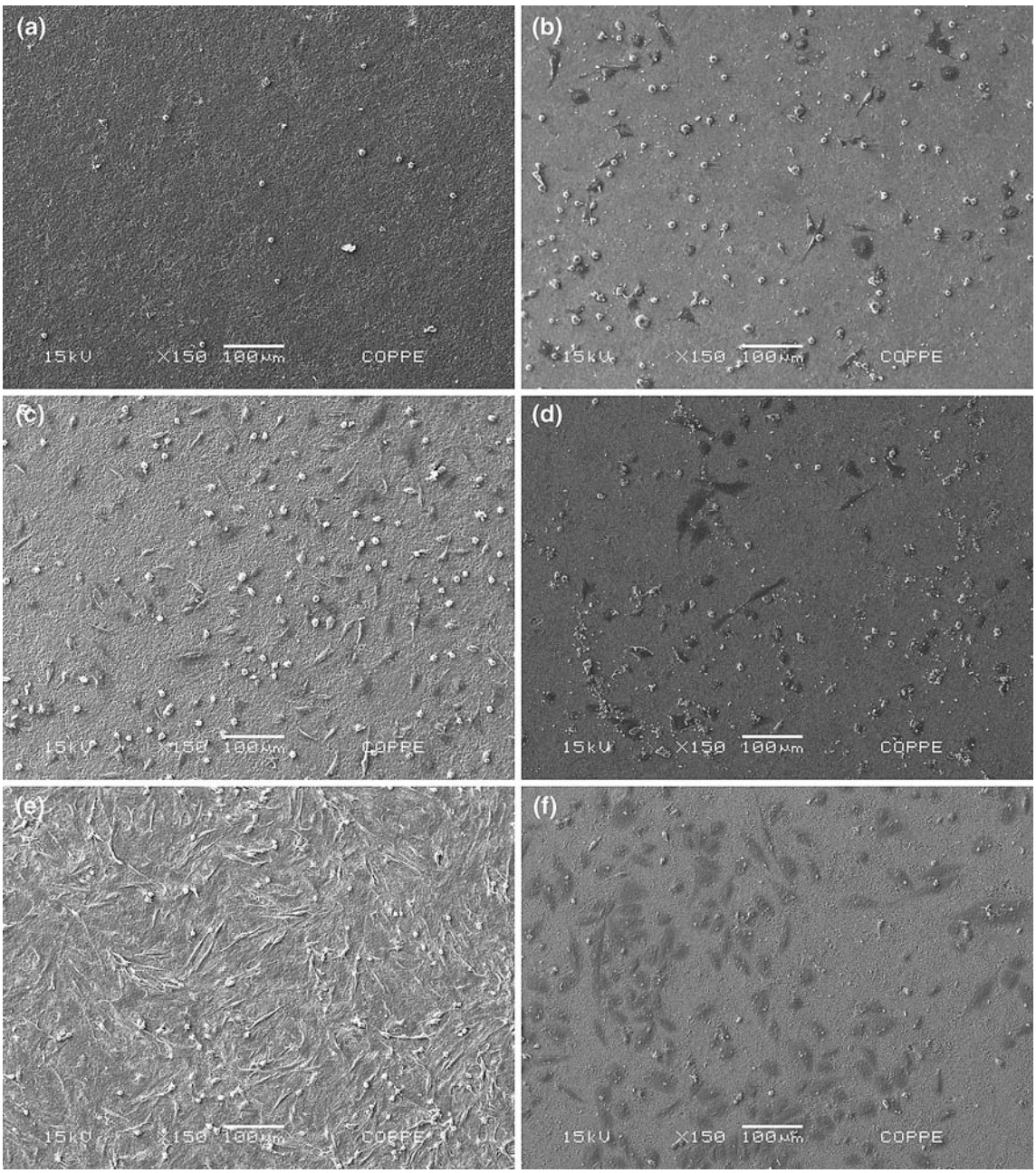

Fig. 6 SEM images of human osteoblast cells (SaOs2) after 4 h, 24 h and 7 days of incubation on β-TCMP (**a**, **c** and **e**) and on β-TCP (**b**, **d**, and **f**), respectively

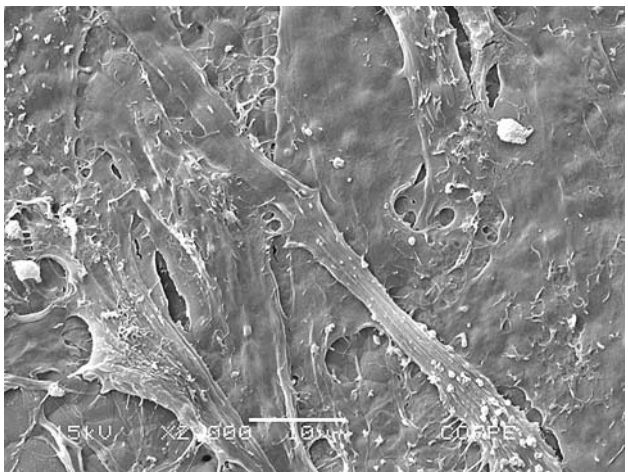

Fig. 7 SEM image of human osteoblast cells (SaOs2) after 7 days of incubation on β-TCMP tablet

receptors that belong to the integrin superfamily [17]. Cells can bind via integrin directly to the implant surface and the integrin expression can be modulated by surface chemistry modification. The modification of the bioceramic surface with Mg^{2+} ions may exert a target for integrin receptors intracellular signaling, which is fundamental for stabilization of osteogenic phenotype. Mg has a direct effect on cell activity: it is mitogenic for osteoblasts in culture and its depletion cause cellular growth inhibition in vitro [18]. Ryan et al. [19] also reported that magnesian-whitlockite stimulated cell proliferation and the synthesis and secretion of collagen. Landi et al. [20] demonstrated greater osteoconductivity and higher material resorption for synthetic Mg-doped hydroxyapatite, (Mg-HA) when compared with pure HA. Mg-HA showed more favorable conditions for bone growth due to the surface characteristics such as composition and nanodimensions.

Comparing the behavior of dense HA with dense β-TCP, Santos et al. [15] concluded that the nanotopography of these calcium phosphates strongly affected the protein adsorption process, being more important than calcium phosphate chemistry. Moreover, the nanotopography exhibited by HA samples (with small grain size) was more favorable to albumin and fibronectin adsorption than the one of β-TCP (with larger grain size). Perhaps the effect of Mg in promoting a dense surface can be another way to justify the higher cell proliferation observed on β-TCMP tablets.

4 Conclusion

Dense tablets of magnesium substituted tricalcium phosphate (β-TCMP), $(Ca, Mg)_3(PO_4)_2$, were successfully obtained by sintering Mg-calcium deficient apatite, prepared by wet chemical synthesis, at 1,000°C for 4 h. β-TCMP tablets showed a dense structure with low microporosity compared to commercial β-TCP tablets.

Higher cell proliferation of human osteoblast cells was stimulated by β-TCMP compared to β-TCP. These preliminary data demonstrate that β-TCMP can support the adhesion and proliferation of human osteoblast cells. Consequently, the magnesium incorporation on calcium deficient apatites followed by sintering at 1,000°C seems to be a useful path to obtain biocompatible and non-cytotoxic dense tablets with TCP structure with potential application on bone engineering.

Acknowledgments The authors acknowledge the financial support given by CNPq, CAPES and FAPERJ. We thank J. C. Araújo, V. C. A. Moraes and E. L. Moreira for Rietveld analyses contribution and the Chemistry Institute of the Federal University of Rio de Janeiro for the FTIR analyses.

References

1. I.R. Gibson, I. Rehman, S.M. Best, W. Bonfield, J. Mater. Sci.: Mater. Med. **12**, 799 (2000). doi:10.1023/A:1008905613182
2. R.Z. LeGeros, in *Calcium Phosphates in Oral Biology and Medicine, Monographs in Oral Sciences*, vol. 15, ed. by H. Myers (Basel, Switzerland, 1991)
3. C. Rey, V. Renugopalkrishan, B.I. Collins, M.J. Glimcher, Calc. Tissue Int **49**, 251 (1991)
4. R.Z. LeGeros, S. Lin, R. Rohanizadeh, D. Mihjares, J.P. LeGeros, J. Mater. Sci.: Mater. Med **14**, 201 (2003). doi:10.1023/A:1022872421333
5. P.N. Kumta, C. Sfeir, D.-H. Lee, D. Olton, N. Choi, Acta. Biomater. **1**, 65 (2005). doi:10.1016/j.actbio.2004.09.008
6. E. Landi, A. Tampieri, M. Mattioli-Belmonte, G. Celotti, M. Sandri, A. Gigante, P. Fava, G. Biagini, J. Eur. Ceram. Soc. **26**, 2593 (2005). doi:10.1016/j.jeurceramsoc.2005.06.040
7. L.W. Schroeder, B. Dickens, W.E. Brown, J. Solid State Chem. **22**, 253 (1977). doi:10.1016/0022-4596(77)90002-0
8. G. Daculsi, R.Z. LeGeros, D. Mitre, Calcif. Tissue Int. **45**, 95 (1989). doi:10.1007/BF02561408
9. B. Wopenka, J.D. Pasteris, Mater. Sci. Eng. C **25**, 131 (2005). doi:10.1016/j.msec.2005.01.008
10. R.Z. LeGeros, A.M. Gatti, R. Kijkowska, D.Q. Mijares, J.P. LeGeros, Key Eng. Mater. **254–256**, 127 (2004)
11. S. Kannan, J.M. Ventura, J.M.F. Ferreira, Ceram. Int. **33**, 637 (2007). doi:10.1016/j.ceramint.2005.11.014
12. H. Zreiqat, C.R. Howlett, A. Zannettino, P. Evans et al., J. Biomed. Mater. Res. **62**, 175 (2002). doi:10.1002/jbm.10270
13. Y. Yamasaki, Y. Yoshida, M. Okazaki, A. Shimazu et al. Biomaterials 24v4913 (2003)
14. J.D. Pasteris, B. Wopenka, J.J. Freeman, K. Rogers, E. Valsami-Jones, J.A.M. van der Houwen, M.J. Silva, Biomaterials **25**, 229 (2004). doi:10.1016/S0142-9612(03)00487-3
15. E.A. dos Santos, M. Farina, G.A. Soares, K. Anselme, J. Mater. Sci.: Mater. Med. **19**, 2307 (2008). doi:10.1007/s10856-007-3347-4
16. K. Lin, J. Chang, J. Lu, W. Wu, Y. Zeng, Ceram. Int. **33**, 979 (2007). doi:10.1016/j.ceramint.2006.02.011
17. G. Gronowicz, M.B. MacCarthy, J. Orthop. Res. **14**, 878 (1996). doi:10.1002/jor.1100140606

18. R.K. Rude, H.E. Gruber, J. Nutr. Biochem. **15**, 710 (2004). doi: 10.1016/j.jnutbio.2004.08.001
19. L.M. Ryan, H.S. Cheung, R.Z. LeGeros, I.V. Kurup, J. Toth, P.R. Westfall, G.M. McCarthy, Calcif. Tissue Int. **65**, 374 (1999). doi: 10.1007/s002239900716
20. E. Landi, G. Logroscino, L. Proietti, A. Tampieri, M. Sandri, S. Sprio, J. Mater. Sci.: Mater. Med. **19**, 239 (2008). doi:10.1007/s10856-006-0032-y